ISBN number for HWRS 2022 is 978-1-925627-64-0

Hydraulics of a broad-crested weir with rounded edges: physical Modelling

Sunhanut Chaokitka and Hubert Chanson

The University of Queensland, School of Civil Engineering, Brisbane QLD 4072, Australia

Email: h.chanson@uq.edu.au

ABSTRACT

A broad-crested weir is a type of weir with a flat crest. It is mainly used to measure the discharge and to act as a hydraulic control. Detailed measurements of free-surface profiles, velocity and pressure profiles, and boundary shear stress were conducted on a large-sized broad-crested weir with rounded corners on both ends. The result showed a rapid redistribution of velocity and pressure profile. It highlighted the effect of the rounded corner at the downstream end on the pressure field. Considering non-uniform velocity profiles and non-hydrostatic pressure distributions, the water depth and momentum correction coefficients suggested that the flow was critical from $0 \le x/L_{crest} \le 1$*. A developing boundary layer was observed from the velocity profiles. The dimensionless boundary shear stress* $\tau_o/\rho g H_1$ *varied from 0.00003 to 0.01. The shear stress increased as the flow accelerated towards the brink of the weir. Across the width of the crest, the shear stress was relatively uniform near the centreline, while larger variations were seen next to the wall. This confirmed the quasi-two-dimensional boundary shear map and the symmetry of the effect from the sidewall on the boundary shear stress of this specific facility.*

INTRODUCTION

A broad-crested weir is a type of weir with a flat crest that is significantly longer than the specific energy, for the streamlines above the crest to be parallel to the crest, i.e. straight, to achieve the near-hydrostatic pressure distributions (Henderson 1966, Chanson 2004). Typically, the dimensionless head above crest H_1/L_{crest} should be between 0.1 and 0.50, with H_1 the upstream head above crest and L_{crest} the weir crest length (Fig. 1) (Govinda Rao and Muralidhar 1963, Bos 1976). The relationship between discharge and head above crest is usually expressed as in a modified form of the Bernoulli principle:

$$Q = C_D \times B \times \sqrt{g} \times \left(\frac{2}{3} \times H_1\right)^{3/2} \qquad (1)$$

with B the crest width, g the gravity acceleration and C_D a dimensionless discharge coefficient. C_D is typically slightly less than unity for a broad-crested weir, although the value might differ between different inflow conditions (Ramamurthy et al. 1988, Gonzalez and Chanson 2007, Sargison and Percy 2009).

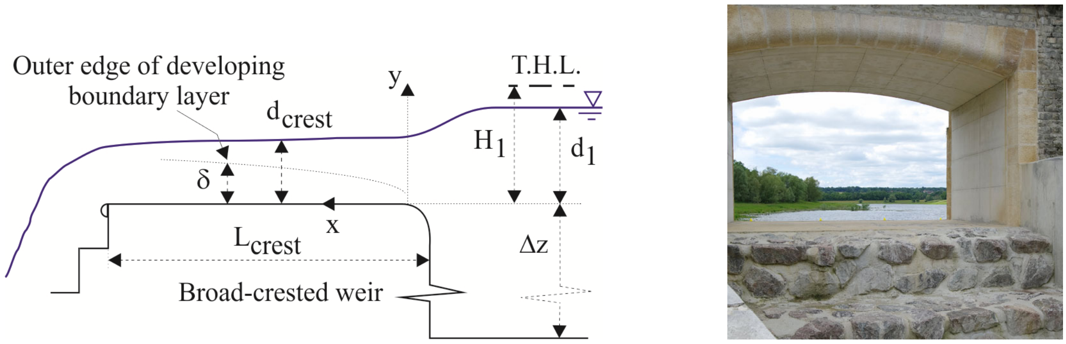

Figure 1. Broad-crest weir: definition sketch (Left) and prototype looking upstream with the reservoir in background (Chazilly dam, France on 6 June 2022) (Right).

The present contribution aims to detail the flow characteristics on a broad-crested weir with rounded edges. Physical measurements were conducted in a large-size facility, with the aim for a systematic characterisation of the free surface profile, velocity and pressure distributions, and boundary shear stress. The study was focused on the two- and three-dimensional flow field.

EXPERIMENTAL FACILITY AND INSTRUMENTATION

This experiment was conducted in the Hydraulics Laboratory at the University of Queensland, in a new facility. The water flow was delivered by three adjustable altering currents (AC) pumps into the 1.7 m deep and 5 m wide intake basin, equipped with a series of baffles and flow straighteners. The discharge was smoothly converged by 2.8 m long smooth symmetrical sidewalls with a converging ratio 5.08:1, resulting in a waveless flow into the test section. The broad-crested weir was installed in a 0.985 m wide acrylic-sidewalled test section (Fig. 2). The weir crest was 0.542 m long with a PVC invert and rounded ends. The upstream wall was vertical and 1.4 m high. The radius of the upstream rounding was 0.058 m, while the downstream rounding had a 0.012 m radius with 180° bend, as sketched in Figure 1. The weir ended with a 1.4 m high steep (1V:0.8H) chute.

The upstream water depth was measured with a pointer gauge connected to a MeasumaX™ single column digital height gauge with an accuracy of ±0.05 mm. The water depth above the crest was measured with three systems: a rail-mounted pointer gauge, a sidewall ruler and sideview photography, with an accuracy of ±0.5 mm. The velocity and pressure measurements were performed with a 3.1 mm thick stainless steel Dwyer® series 160 Prandtl-Pitot tube, featuring four 0.51 mm diameter static openings, 25.4 mm behind the 1.19 mm diameter dynamic tapping. The translation of the Prandtl-Pitot probe in the vertical direction was measured by a Mitutoyo™ digital scale unit with an accuracy of ±0.025 mm, and the horizontal translation was recorded with an accuracy of ±1 mm. The boundary shear stress was measured using the Prandtl-Pitot tube lying on the invert. Using Prandtl mixing length theory, the boundary shear stress τ_o may be related to the velocity reading V_b:

(2) $$\tau_o = \rho \times \left(\kappa \times \frac{V_b}{N} \right)^2$$

where ρ is the fluid density, κ = 0.4 is the von Karman constant, N = 7 for smooth turbulent boundary layer, and V_b is velocity next to the boundary (Cabonce et al. 2017,2019).

Further observations were taken with an iPhone Xs and a dSLR Pentax™ K-3 camera.

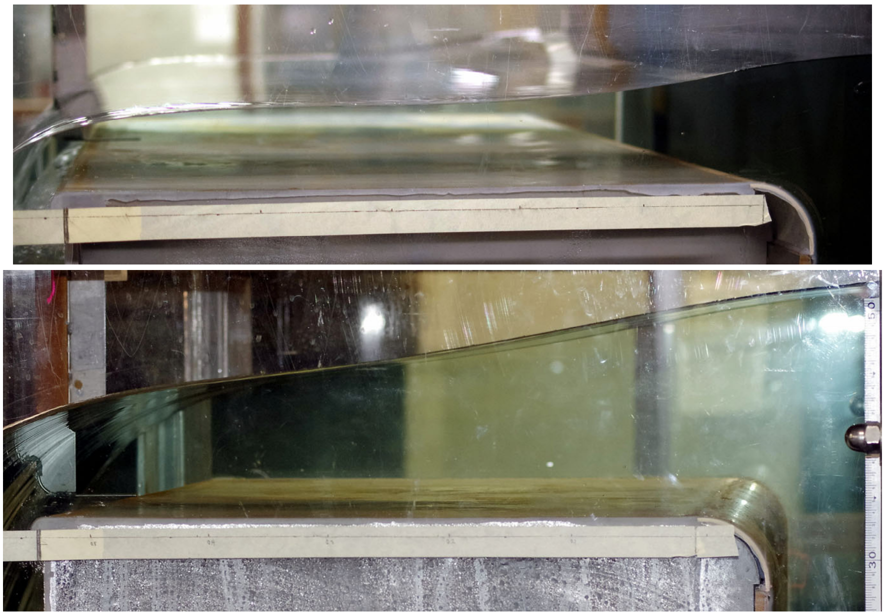

Figure 2. Broad-crested weir overflow for H_1 = 0.11 m (Top) and H_1 = 0.20 m (Bottom). Flow direction from right to left

BASIC RESULTS

Flow patterns

For all experiments, i.e. $H_1 < 0.25$ m, the upstream flow was quiescent. The water accelerated over the broad crest and was supercritical on the downstream steep slope. Figure 2 illustrates two typical flow conditions. Dye injection showed that the streamlines were nearly parallel to the invert about the middle section of the crest, while streamline curvature was observed at both upstream and downstream ends. As the flow passed over the crest, the water depth gradually decreased. The downstream rounding forced the stream to bend downwards into the 1V:0.8H steep channel, as reported by Zhang and Chanson (2015) for a 1V:1H slope.

The free surface profiles were recorded for several upstream heads above crest: $0.2 \le H_1/L_{crest} \le 0.437$. Typical data sets are reported in Figure 3, showing a good agreement between two different measurement techniques. While the water surface was flat in the middle of the crest, the curvature of the surface was relatively high in the vicinity of both ends of the broad crest (Fig. 3).

At low discharges, the water depth was relatively constant along the crest, before rapidly decreasing at the downstream end of the weir. At high discharges, in contrast, the longitudinal free-surface profile was not parallel to the invert at any point along the length of the weir. These patterns were consistent with previous studies (e.g., Felder and Chanson 2012, Zhang and Chanson 2016).

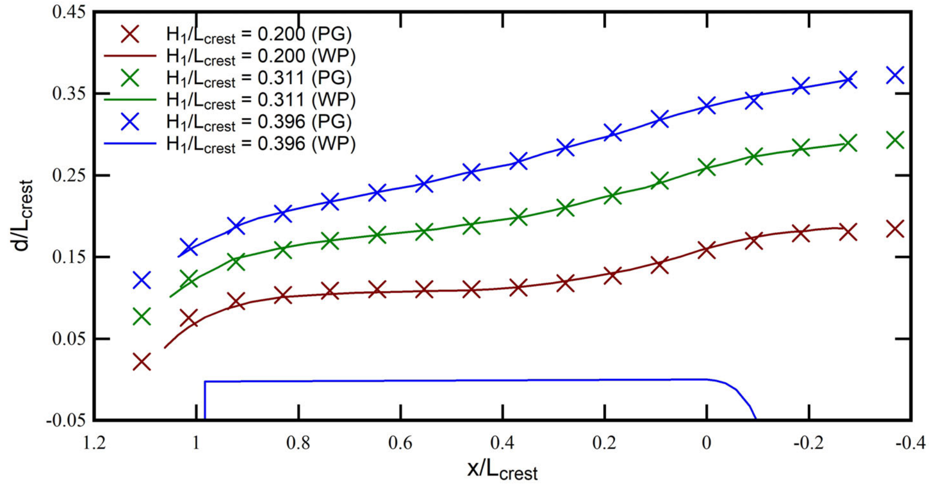

Figure 3. Longitudinal free-surface profiles above the broad-crested weir: comparison between centreline point gauge (PG) and sideview imaging (WP) data.

Pressure and velocity distributions

Detailed velocity and pressure measurements were conducted on the broad-crested weir along its centreline, for upstream heads above crest H_1 = 0.110 m, 0.150 m, 0.200 m and 0.235 m, corresponding to $0.20 < H_1/L_{crest} < 0.45$. For each set of flow conditions, seven vertical profiles were recorded along the crest. Figure 4 shows some typical pressure and velocity distributions.

For all flow conditions, the data sets showed some major redistribution of the velocity and pressure profiles from the upstream end to the downstream end (Fig. 4). For $0.185 < x/L_{crest} < 0.738$, the velocity profiles resembled typical velocity profile in an open channel, with zero at the invert and a monotonically increasing velocity towards the free surface. At the leading and trailing edges of the weir, however, the velocity profiles were different, and the maximum velocity instead occurred towards the mid-water column, because of the streamline curvature. Similarly, the pressure distributions were hydrostatic about the mid-section of the weir crest, but departed from the hydrostatic pressure profile at both ends (Fig. 4).

The longitudinal distributions of velocities indicated the development of a bottom boundary layer. The finding was consistent with previous studies in relatively large-size facilities (Gonzalez and Chanson 2007, Felder and Chanson 2012, Zhang and Chanson 2016).

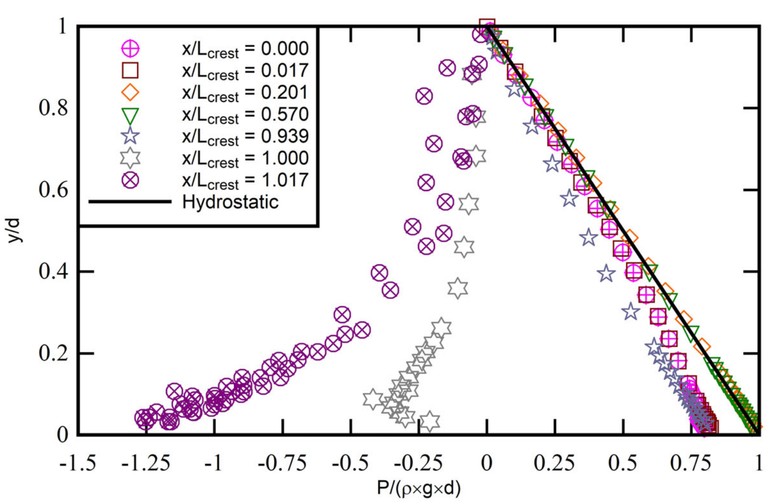

(A)

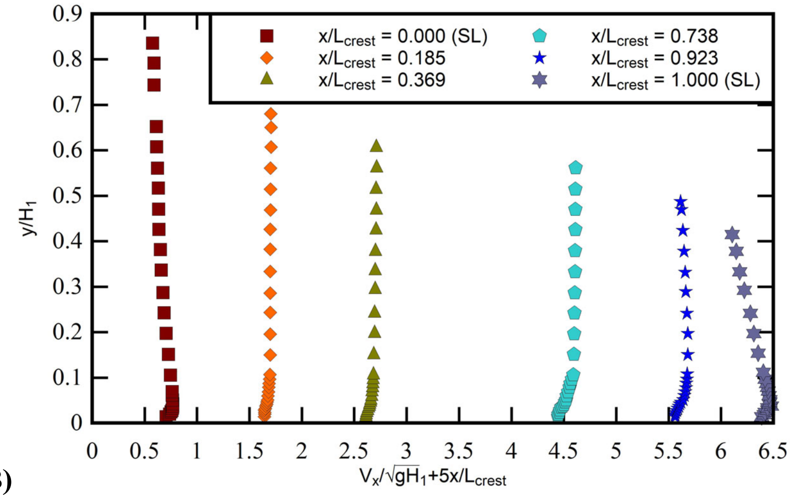

(B)

Figure 4. Vertical pressure and velocity distributions above the broad-crested weir on the centreline. (A) Pressure distributions for H_1 = 0.11 m. (B) Velocity distributions for H_1 = 0.11 m.

BOUNDARY SHEAR STRESS MEASUREMENTS

On the crest invert, the skin friction boundary shear stress was derived from the velocity gradient next to the invert (Eq. (2)). Typical centreline data sets are presented in Figure 5A. For a given upstream head, the general trend showed a monotically increasing shear stress from the upstream end to the downstream end of the crest. And, about the middle section of the crest invert, the data indicated a very gentle growth along $0.2 < x/L_{crest} < 0.8$. The data set showed further that the increased rate in shear force was positively correlated to the upstream head H_1/L_{crest}. For $0.20 < H_1/L_{crest} < 0.45$. the dimensionless boundary shear stresses $\tau_o/(\rho\times g\times H_1)$ varied longitudinally between 0.00003 and 0.01, which would correspond to Darcy-Weisbach friction factors between 0.001 and 0.3, on the crest centreline. Quantitatively, the results were comparable to the calculations of Felder and Chanson (2012) using different approaches, namely logarithmic law and momentum integral equation data, although the latter approaches are more time-consuming and no more accurate.

The boundary shear stress was further measured across the width of the broad crest at several longitudinal locations. Typical data are shown in Figure 5B for H_1/L_{crest} = 0.277. Despite some fluctuations, the shear stress was reasonably uniformly distributed across the width. Some sidewall effects were seen, with a local maximum in shear stress next to the sidewalls. The impact of the sidewall on the boundary shear stress was quite symmetrical about the centreline on both sides. It is believed that the local maximum in boundary shear stress was linked to the formation of elongated vortices with streamwise axis in the bottom corners. These eddies originated most likely in the form the corner eddies immediately upstream of the vertical upstream wall of the weir. Such "spiral vortices" were illustrated by Rouse (1938, pp. 75 & 271) and Gonzalez and Chanson (2007, p.109), and resulted from secondary flow motion at the base of the weir with the strongest effects next to the corners. Dye injection above the broad-crest showed the continuing eddy coherence in the weir's broad crest corners.

Altogether, the transverse distributions of boundary shear stress on the broad-crested weir differed from the experimental observations in straight rectangular channels (Prandtl 1952, Chanson 2014).

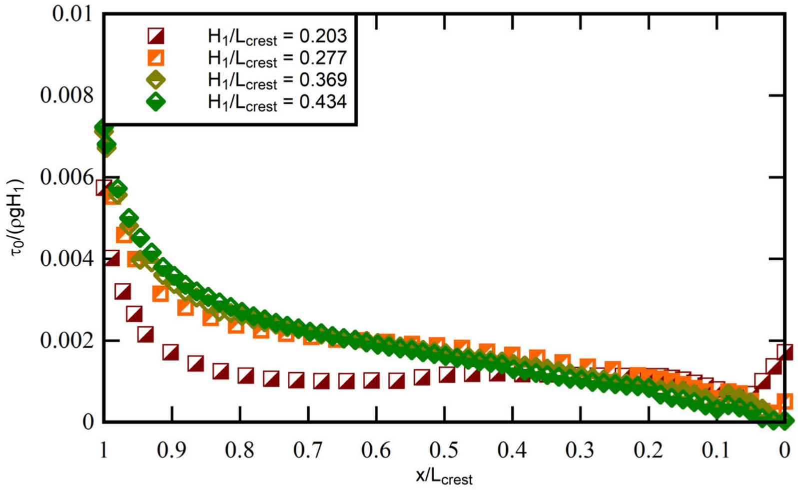

(A)

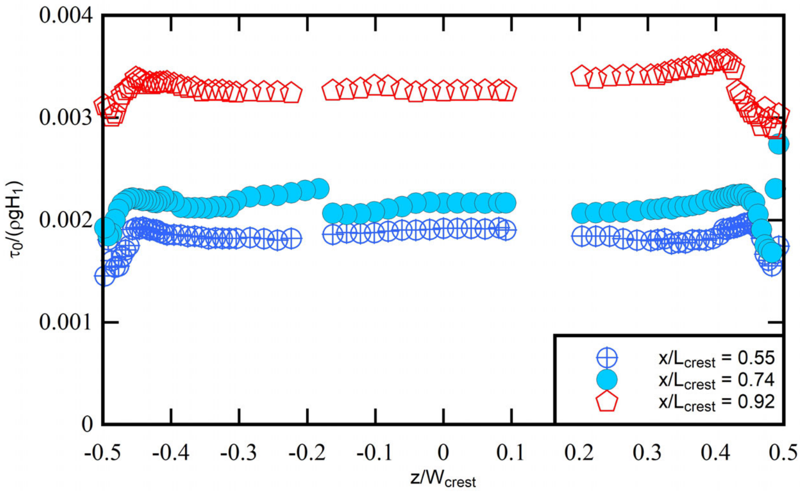

(B)

Figure 5. Boundary shear stress distributions on the broad-crested weir. (A) Longitudinal distributions on the weir centreline. (B) Transverse distributions for H_1/L_{crest} = 0.277.

DISCUSSION

Discharge coefficient

The dimensionless discharge coefficient was derived from Equation (1), with the unit discharge calculated from the velocity measurements above the crest:

$$\text{(3)} \qquad \frac{Q}{B} = \int_{z=0}^{d} V \times dz$$

at x/L_{crest} = 0.55. For the present investigation, the discharge coefficient C_D was approximately a linear function of the head ratio H_1/L_{crest}:

$$\text{(4)} \qquad C_D = 0.901 + 0.256 \times \frac{H_1}{L_{crest}} \qquad \text{for } 0.2 < H_1/L_{crest} < 0.45$$

The present data are reported in Figure 6, in which they are compared to earlier data sets of broad-crested weirs with rounded edges (Bazin 1896, Bos 1976, Felder and Chanson 2012, Zhang and Chanson 2016). For H_1/L_{crest} > 0.4, the discharge coefficient data were greater than unity, indicating that the weir crest was no more "long enough" for the streamlines to be parallel to the crest invert and the pressure distributions to be hydrostatic above the crest. Altogether, the dimensionless discharge coefficient positively correlated to the upstream head ratio, as shown in Figure 6 and estimated by Equation (4).

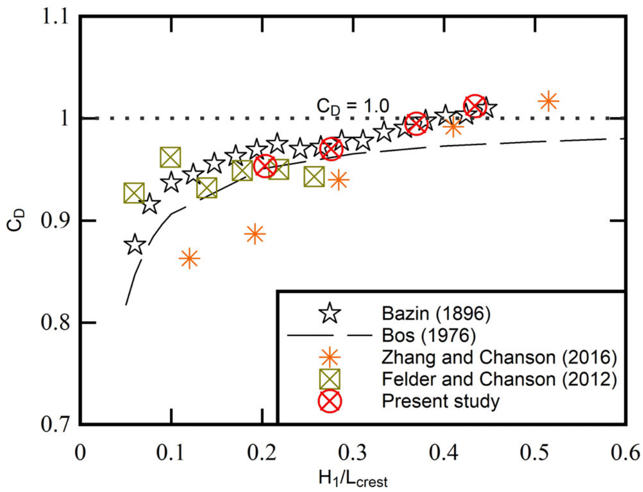

Figure 6. Dimensionless discharge coefficient above a broad-crested weir with rounded edges. Comparison between present study and earlier data sets (Bazin 1896, Bos 1976, Felder and Chanson 2012, Zhang and Chanson 2016).

Critical flow conditions

In open channel flows, critical flow conditions are defined when the specific energy is minimum (Bakhmeteff 1912,1932, Henderson 1966). By definition, the specific energy is minimum above the highest point of a spillway crest, and critical flow conditions should occur everywhere along a broad-crested weir.

For a smooth, frictionless flow, a detailed solution of the critical flow conditions was proposed for open channel flow situations with non-hydrostatic pressure distributions and non-uniform velocity distributions (Liggett 1993, Chanson 2006). Simply, at critical flow conditions, there is a unique relationship between the pressure coefficient Λ, the velocity correction coefficient β, and the dimensionless discharge coefficient C_D for a given discharge per unit width Q/B and minimum specific energy E_{min}, with

(5) $$\Lambda = \frac{1}{2} + \frac{1}{d} \times \int_{z=0}^{d} \frac{P}{\rho \times g \times d} \times dz$$

(6) $$\beta = \frac{d}{q^2} \times \int_{z=0}^{d} V^2 \times dz$$

Together with the continuity equation, the minimum specific energy condition yields a relationship between the ratio d_c/E_{min} of critical depth to minimum specific energy in the form of a third-degree polynomial function (Chanson 2006):

(7) $$X^3 - \frac{1}{\Lambda} \times X^2 + \frac{1}{2} \times \left(\frac{2}{3}\right)^3 \times \frac{\beta \times C_D^{\ 2}}{\Lambda} = 0 \qquad \text{with } X = \frac{d_c}{E_{min}}$$

in which d_c is the most general expression of the critical depth for nonhydrostatic pressure distribution and non-uniform velocity distribution. The analytical solution was thoroughly tested with circular weir, parabolic weir, broad-crested weir and undular flow data sets in steady and unsteady flows (Chanson 2008, Castro-Orgaz and Chanson 2016). The present data are shown in Figure 7, in which the present results followed relatively closely the solutions S1 and S3 (Chanson 2006). Herein, the coefficients Λ and β were calculated based upon the pressure and velocity measurements respectively. The comparative presentation showed further a change in solution depending upon the longitudinal location x/L_{crest} (Fig. 7).

Implicitly, the present finding confirmed that the flow was critical above the entire broad-crest, even when the pressures were not hydrostatic and the velocity profiles non uniform. It is acknowledged that there is a few data scatter, possibly linked to some limitation of the approximation of no-energy-loss which would not be valid anywhere. Indeed, the observed bottom boundary layer development implied some boundary friction and associated friction losses, while the local shear stress maxima next to the walls indicated some strong secondary motion there.

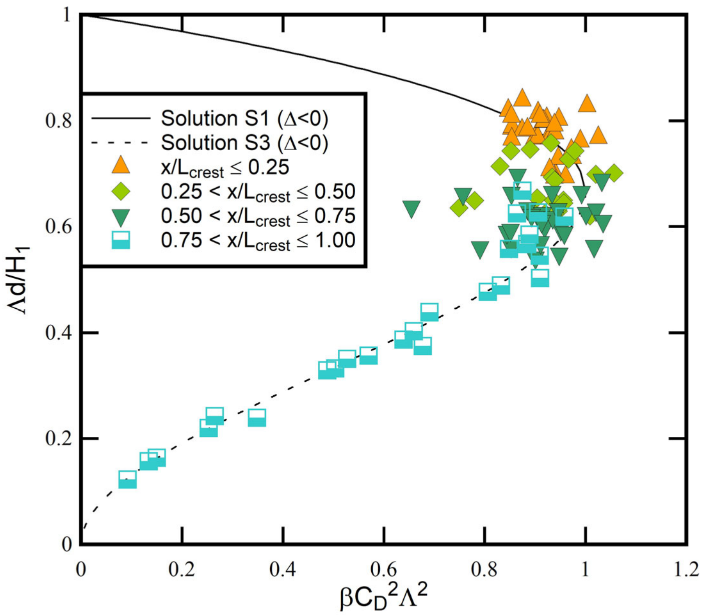

Figure 7. Dimensionless relationship between critical depth and discharge coefficient above broad-crested weir with rounded edges. Data sets: Present study, Felder and Chanson (2012), Zhang and Chanson (2016).

CONCLUSION

New physical experiments were performed in the overflow on a large broad-crested weir with rounded edges. The flow properties were thoroughly documented using a Prandtl-Pitot tube, and the data sets included pressure, velocity and boundary shear stress distributions. The data were overall in agreement with the literature for $0.20 < H_1/L_{crest} < 0.45$. Longitudinally, the dimensionless boundary shear stresses varied within $0.00003 < \tau_o/(\rho \times g \times H_1) < 0.01$ on the crest centreline, corresponding to Darcy-Weisbach friction factors from 0.001 to 0.3. The transverse distributions of boundary shear stress were quasi-uniform, and presented some local maxima next to the sidewalls. These shear stress maxima were likely caused by elongated tornado-liked eddies issued from the bottom of the weir upstream wall.

Critical flow conditions occurred along the whole weir crest length, despite the non-hydrostatic pressure distributions and non-uniform velocity profiles. Marked deviations were indeed observed at both ends of the weir crest, linked to the rapid redistributions of velocity and pressure fields.

In summary, the present data set was conducted in a relatively large-size facility, ensuring that the results can be extrapolated to full-scale prototypes with negligible scale effects. They confirmed the range of dimensionless discharge coefficients for broad-crested weir with rounded edges. They further hinted the importance of the upstream approach flow conditions and inflow channel geometry, with implications on the three-dimensionality of the weir overflow motion, e.g. in terms of boundary shear stresses.

ACKNOWLEDGEMENTS

The authors acknowledge the technical assistance of Jason Van Der Gevel and Stewart Matthews (The University of Queensland). The financial support of the first author through the 2021-2022 UQ Summer Research Program is acknowledged.

REFERENCES

Bakhmeteff, B.A. (1912). "*O Neravnomernom Dwijenii Jidkosti v Otkrytom Rusle*." ('Varied Flow in Open Channel.') St Petersburg, Russia (in Russian).

Bakhmeteff, B.A. (1932). "*Hydraulics of Open Channels*." McGraw-Hill, New York, USA, 1st ed., 329 pages.

Bazin, H. (1896). "Expériences nouvelles sur l'ecoulement par déversoir." ('Recent experiments on the flow of water over weirs.') *Mémoires et Documents, Annales des Ponts et Chaussées*, Paris, France, Sér. 7, Vol. 12, 2nd Sem., 645–731 Plates (in French).

Bos, M.G. (1976). "*Discharge Measurement Structures*." Publication No. 161, Delft Hydraulic Laboratory, Delft, The Netherlands.

Cabonce, J., Fernando, R., Wang, H., and Chanson, H. (2017). "Using Triangular Baffles to Facilitate Upstream Fish Passage in Box Culverts: Physical Modelling." *Hydraulic Model Report No. CH107/17*, School of Civil Engineering, The University of Queensland, Brisbane, Australia, 130 pages

Cabonce, J., Fernando, R., Wang, H., and Chanson, H. (2019). "Using Small Triangular Baffles to Facilitate Upstream Fish Passage in Standard Box Culverts." *Environmental Fluid Mechanics*, Vol. 19, No. 1, pp. 157–179 (DOI: 10.1007/s10652-018-9604-x).

Castro-Orgaz, O., and Chanson, H. (2016). "Minimum Specific Energy and Transcritical Flow in Unsteady Open-Channel Flow." *Journal of Irrigation and Drainage Engineering*, ASCE, Vol. 142, No. 1, Paper 04015030, 12 pages (DOI: 10.1061/(ASCE)IR.1943-4774.0000926).

Chanson, H. (2004). "*The Hydraulics of Open Channel Flow: An Introduction*." Butterworth-Heinemann, 2nd edition, Oxford, UK, 630 pages.

Chanson, H. (2006). "Minimum Specific Energy and Critical Flow Conditions in Open Channels." *Journal of Irrigation and Drainage Engineering*, ASCE, Vol. 132, No. 5, pp. 498-502 (doi:10.1061/(ASCE)0733-9437(2006)132:5(498)).

Chanson, H. (2008). "Minimum Specific Energy and Critical Flow Conditions in Open Channels - Closure." *Journal of Irrigation and Drainage Engineering*, ASCE, Vol. 134, No. 6, pp. 883-887 (DOI: 10.1061/(ASCE)0733-9437(2008)134:6(883)).

Chanson, H. (2014). "*Applied Hydrodynamics: An Introduction*." CRC Press, Taylor & Francis Group, Leiden, The Netherlands, 448 pages & 21 video movies.

Felder, S, and Chanson, H. (2012). "Free-surface Profiles, Velocity and Pressure Distributions on a Broad-Crested Weir: a Physical study." *Journal of Irrigation and Drainage Engineering*, ASCE, Vol. 138, No. 12, pp. 1068–1074 (DOI: 10.1061/(ASCE)IR.1943-4774.0000515).

Govinda Rao, N.S., and Muralidhar, D. (1963). "Discharge Characteristics of Weirs of Finite-Crest

Width." *Journal La Houille Blanche*, Aug./Sept., No. 5, pp. 537-545.

Gonzalez, C.A., and Chanson, H. (2007). "Experimental Measurements of Velocity and Pressure Distribution on a Large Broad-Crested Weir." *Flow Measurement and Instrumentation*, Vol. 18, No. 3-4, pp. 107-113 (DOI 10.1016/j.flowmeasinst.2007.05.005).

Henderson, F.M. (1966). "*Open Channel Flow*." MacMillan Company, New York, USA.

Liggett, J.A. (1993). "Critical Depth, Velocity Profiles and Averaging." *Journal of Irrigation and Drainage Engineering*, ASCE, Vol. 119, No. 2, pp. 416-422.

Prandtl, L. (1952). "*Essentials of Fluid Dynamics with Applications to Hydraulics, Aeronautics, Meteorology and Other Subjects*." Blackie & Son, London, UK, 452 pages.

Ramamurthy, A.S., Tim, U.S., and Rao, M.V.J. (1988). "Characteristics of Square-Edged and Round-Nosed Broad-Crested Weirs." *Journal of Irrigation and Drainage Engineering*, ASCE, Vol. 114, No. 1, pp. 61-73.

Rouse, H. (1938). "*Fluid Mechanics for Hydraulic Engineers*." McGraw-Hill Publ., New York, USA (also Dover Publ., New York, USA, 1961, 422 pages).

Sargison, J.E., and Percy, A. (2009). "Hydraulics of Broad-Crested Weirs with Varying Side Slopes." *Journal of Irrigation and Drainage Engineering*, ASCE, Vol. 135, No. 1, pp. 115-118.

Zhang, G., and Chanson, H. (2015). "Free-Surface and Seepage Bubbly Flows on a Gabion Stepped Spillway Weir: Experimental Observations." *Proc. 36th IAHR World Congress*, The Hague, The Netherlands, 27 June-3 July, Theme 8, pp.6624-6633.

Zhang, G., and Chanson, H. (2016). "Hydraulics of the Developing Flow Region of Stepped Spillways. I: Physical Modeling and Boundary Layer Development." *Journal of Hydraulic Engineering*, ASCE, Vol. 142, No. 7, 8 pages (DOI: 10.1061/(ASCE)HY.1943-7900.0001138).

BIOGRAPHY

Sunhanut Chaokitka is a 3rd-year Civil Engineering undergraduate student at the University of Queensland. Large and magnificent structures got him into the field, but now he enjoys learning about any infrastructure that makes our convenient life possible.

Hubert Chanson is Professor of Civil Engineering at the University of Queensland, where he has been since 1990, having previously enjoyed an industrial career for six years. His main field of expertise is environmental fluid mechanics and hydraulic engineering, both in terms of theoretical fundamentals, physical and numerical modelling. He leads a group of 5-10 researchers, largely targeting flows around hydraulic structures, two-phase (gas-liquid and solid-liquid) free-surface flows, turbulence in steady and unsteady open channel flows, using computation, lab-scale experiments, field work and analysis. He has published over 1,250 peer reviewed publications including two dozen of books. He serves on the editorial boards of International Journal of Multiphase Flow, Flow Measurement and Instrumentation, and Environmental Fluid Mechanics, the latter of which he is currently a senior Editor. His Youtube channel is: {https://www.youtube.com/channel/UCm-SedWAjKdQdGWNbCwppqw}.